DOI: 10.21062/mft.2023.027 © 2023 Manufacturing Technology. All rights reserved. http://www.journalmt.com

Geometric Accuracy of Components Manufactured by SLS Technology Regarding the Orientation of the Model during 3D Printing

Miroslav Matuš (0009-0002-9214-8696)[1], Vladimír Bechný (0000-0002-2372-5974)[1], Richard Joch (0000-0002-9937-0057)[1], Mário Drbúl (0000-0002-8036-1927)[1], Jozef Holubják (0000-0003-3226-9445)[1], Andrej Czán (0000-0002-8826-1832)[1], Martin Novák (0000-0002-2010-4398)[2], Michal Šajgalík (0000-0002-4908-1046)[1]
[1]Faculty of Mechanical Engineering, Žilinská univerzita v Žiline, Univerzitná 8215/1, 010 26 Žilina, Slovakia. E-mail: miroslav.matus@fstroj.uniza.sk
[2]Faculty of Mechanical Engineering, Jan Evangelista Purkyne University in Usti nad Labem, Pasteurova 3334/7, 400 01 Usti nad Labem. Czech Republic.

Selective Laser Sintering (SLS) or sintering of polymer powders is one of the most well-known additive technologies for printing 3D components. The properties of individual polymer powder materials have a significant impact on the quality of the manufactured part. Potential deformation and shrinkage can occur during printing if a significant number of parts are piled on top of one another or are oriented incorrectly, accumulating thermal energy in certain areas. The aforementioned research focuses on an experimental study to investigate the impact of the distribution and orientation of printing samples in the build chamber on the accuracy of dimensions and the surface roughness of PA12 prints. The aim of the study was to examine the impact of model settings during production as well as the effect of individual factors on the properties of manufactured parts, with a focus on ensuring that heat rises evenly from each print without accumulating.

Keywords: Additive Manufacturing, Selective Laser Sintering, Geometric Accuracy, PA12

1 Introduction

Additive manufacturing (AM) is a group of innovative technologies that create objects in the form of digital models through the gradual reinforcement of material layer-by-layer [1,2,23]. According to ISO/ASTM, Powder Bed Fusion (PBF) is classified as one of the seven categories of AM technologies. This technology has a promising future in both industrial and academic organizations due to its capacity to make components with complex geometries and to employ any powder that can be melted or sintered [3,4,24]. As a result of the rapid advancement of additive manufacturing technologies, such as SLS technology, manufactured components are increasingly used in a wide range of industries, even as a source of design features[5]. Despite the available information on the mechanical properties of parts printed from polyamide powders, only the results of the tensile test are declared by material suppliers and manufacturers of production equipment. Additionally, the stated accuracy of production equipment is not reliably declared. The accuracy of the movement of the individual axes is insufficient since several process parameters influence the quality of the manufactured components. Furthermore, there is a lack of information on the orientation of the printed model in the build chamber, the influence of the individual axes of the model setup on the achieved geometric characteristics, and the integrity of the manufactured surface [6,7]. To manufacture a component by additive technology, a 3D model of the component is required. This can be made by scanning a material body or structural design in a CAD system [8]. For a wide range of CAD programs, it is necessary to export the completed 3D model into standard formats such as the stl format. It is vital to pay attention to the export process settings to achieve the required quality of the 3D model. If the quality requirements of the model are not fulfilled, there will be a significant reduction in the accuracy of the component that is built.

Selective Laser Sintering (SLS) is one of the most common powder-based technologies for additive manufacturing. As a result, SLS technology is currently employed in the manufacturing of a wide range of components. Due to the absence of supporting structures, SLS technology can be used for complex-shaped components. With the availability of advanced printing materials, manufactured components can now be used not only for prototype applications but also for mechanically stressed components in real-world conditions. This technology, which is remarkably similar to Stereolitography (SLA), uses powdered materials (plastic, metal, and ceramic) that are fused, or more precisely sintered with a laser beam [9]. High-powered lasers are used in selective laser sintering (SLS) to sinter powder material to create a printed object. This can result in changes to the internal structure of the

object as well as its surface [10,11,12]. The laser hardens the desired shape of the object into solid powder material, which is then applied to the print bed. After one layer has hardened, the machine applies another thin layer of powder, which is then laser-hardened. Finally, the prints with increased strength are obtained but must be carefully cleaned and removed from unhardened dust. Professional machines that utilize the laser sintering principle are used in industrial production and the production of prototypes for functional testing. The fundamental difference is that the final materials are no longer required to be made of plastic but can instead be made directly of metals or other solid materials such as ceramics. [13,14]. The advantages of SLS printing include the ability to position the printed part arbitrarily in the space of the build chamber and the ability to print a series of prototypes in the X, Y, and Z axes using non-sintered powder as support. The disadvantage is the difficulty in achieving typological characteristics that correspond to the CAD model's dimensions while printing multiple parts at once. Furthermore, thermal energy can accumulate in specified places when a more complex part is poorly positioned or when numerous pieces are piled on top of each other, then warping can occur during cooling. [15]

2 Methodology

The main focus of the experiment is the effect of the layout and orientation of the print samples in the print chamber. Emphasis is also placed on the dimensional accuracy and surface roughness of the PA12 prints. The effect of pattern alignment during production, as well as the influence of various factors on the properties of the fabricated parts, were also studied, with a focus on ensuring that heat rises evenly from each printout without accumulation.

2.1 Used material

The semi-crystalline polymer polyamide 12 (PA12) is a strong, durable material that is widely utilized in the medical, automotive, aerospace, and biomedical industries because of its excellent mechanical properties such as good machinability and low porosity. If reprocessing and use of insoluble materials were not possible, low usage of the material in SLS technologies, collection, and disposal of powders would be uneconomical and environmentally harmful. [16] According to research and the latest findings, non-sintered materials are vulnerable to complex thermal and chemical degradation when used repeatedly. [17] Furthermore, the quality of the prints and their mechanical properties are also affected by the SLS printing settings, such as laser power, laser energy density, scan speed, the distance between the hatches and the scan length of the parts. [18]

2.2 Sample Design

The proposed material (Tab. 1) for printing the test model (Fig. 1) was polyamide black powder, which is suitable for functional prototypes, and chemically resistant products. Furthermore, it has high-temperature resistance. The model's dimensions are 25x10 mm, and its thickness is 10 mm. During printing, the new PA12 Smooth-30% powder is mixed in the prescribed ratio with 70% of the used powder. The amount of fresh powder needed is calculated by the software Sinterit Studio. [19]

Tab. 1 *Properties of the material PA12 [19]*

Property	Value
Particle size (μm)	18-19
Tensile Strength (MPa)	41
Melting point (°C)	182
Roughness Ra top surface (μm)	9.680
Roughness Ra side surface (μm)	6.470
Roughness Rz top surface (μm)	31.633
Roughness Rz side surface (μm)	54.184
Impact strength (KJ/m²)	15-20
Printout density (g/cm³)	1.0

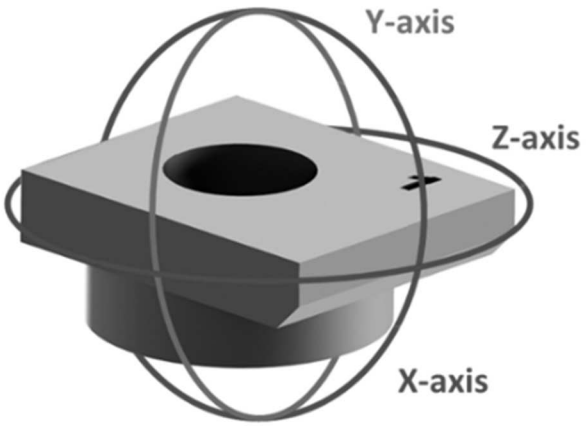

Fig. 1 *Model of the sample*

The software product Minitab 2020 used for the orientation of prints in the build chamber is equipped with several analytical and graphical tools that can be used to better understand the results. Design of experiments method (DOE) identifies process conditions and print components that influence quality. Subsequently, the settings of the parameters that optimize the outcomes can be determined. [20] An experiment was carried out based on the developed DOE proposal, which included 17 samples of repeating five values in X, Y, and Z coordinates (Tab. 2).

Tab. 2 *Repeataing values when designing using DOE*

Angle adjustment			
Number	X	Y	Z
1	0	0	0
2	90	0	0
3	0	90	0
4	90	90	0
5	0	0	90
6	90	0	90
7	0	90	90
8	90	90	90
9	22.5	45	45
10	67.5	45	45
11	45	22.5	45
12	45	67.5	45
13	45	45	22.5
14	45	45	67.5
15	45	45	45
16	45	45	45
17	45	45	45

2.3 SLS parameters

Using Sinterit studio, it is possible not only to adjust the height of the printed layer and the laser power ratio but also to optimize the entire printing process and thereby achieve better properties of the printed model.

Tab. 3 *Print parameters data*

Property	Value
Laser power ratio	1.0
Layer height setting(mm)	0.100
Camber temperature (°C)	178

2.4 Measurement methodology

The surface roughness of injection molded parts is determined by the quality of the mold surface. It is 0.012-0.025 μm for super high gloss and 3.20-18.0 μm for matte texture finish. In previous experiments, typical surface roughness values for the SLS process ranged from 5 to 25 μm. [21]

To evaluate the quality of the 3D surface roughness, two roughness height parameters (Sa - the arithmetical mean height of the tested area and Sz - the maximum height of the tested area) were measured for the printed samples. A non-contact Alicona InfiniteFocus G5 device was used to measure the surface roughness of the samples. This measuring system allows for a detailed 3D surface analysis, including 3D colour images (Fig.6) with a high vertical resolution of up to 0.01 μm and a precise measurement analysis ranging from simple dimensions data to 2D Ra and 3D surface roughness. [22] The measured surfaces (Fig. 2) are area A - the top part of the sample (SaA, SzA) and area B - the side part of the sample (SaB, SzB).

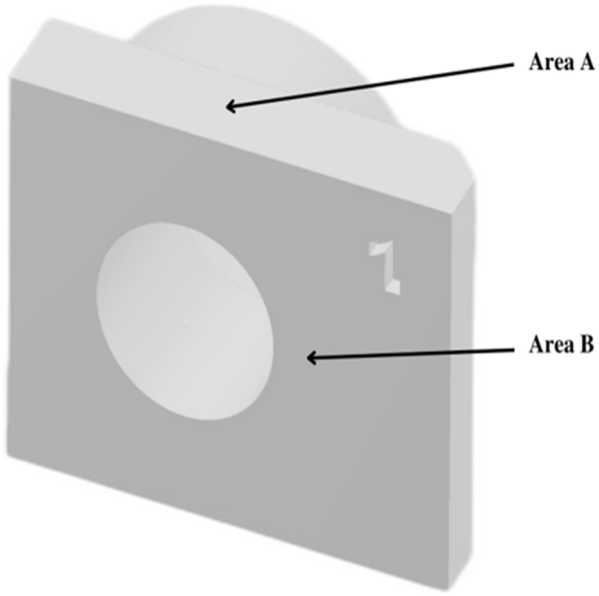

Fig. 2 *Surface roughness measurement of the sample areas*

Dimensional accuracy was measured using the two-point measurement method in addition to surface roughness. For 2D measurement, a micrometer, MAHR Micromar 40 EWR, and the dimensions 25x20x10 were employed (Fig.2).

3 Results

Two surface roughness height parameters, Sa and Sz, were selected to determine the surface quality of the planar (3D) roughness characteristics. These parameters represent a group of surface texture parameters where the statistical characteristics of the height z (x,y) are evaluated.

3.1 Surface Evaluation

Based on the graphical representation of the measured values of the parameter Sa (Fig. 3) over area A, the roughness of all samples was nearly identical. Samples 6,9,11 showed increased roughness, and within area B a higher roughness was recorded for samples 2,8,9,10,11. The highest roughness was shown by sample 12 with a similar value within areas A and B. Area A achieved overall better results than area B. Samples that had significant differences in measured values were not considered during the evaluation. According to the Sa parameter, samples with an orientation of 90° and 45° in any axis and an average SaA value of 13.45 m are optimal for achieving the most stable roughness.

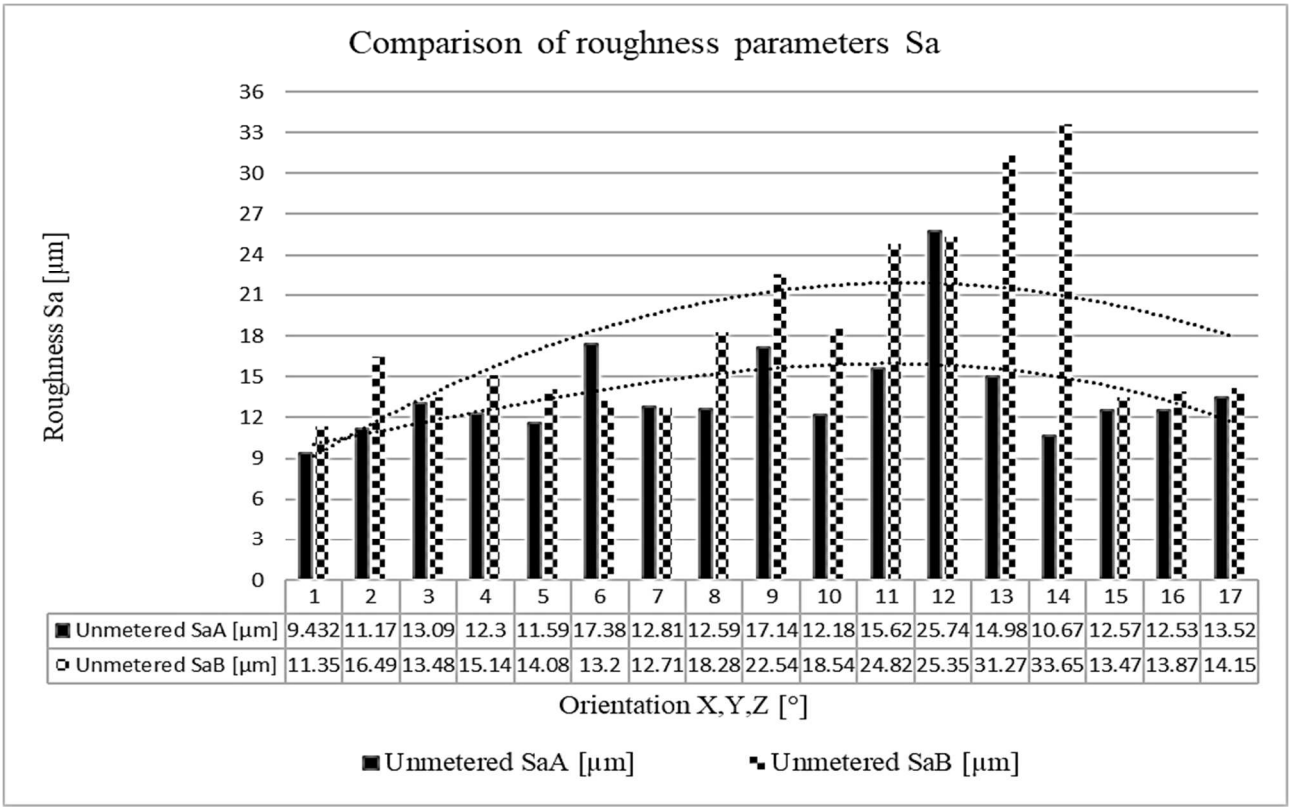

Fig. 3 *Graphical comparison of the results of measuring samples of the roughness parameter Sa*

The measured values (Fig. 4) reach a comparable roughness Sz. Due to measurement inaccuracy and deviations induced by non-sintered powder, the highest parameter in the measured area B for sample 1 was not considered. The best parameters were achieved by samples that were oriented by 90° and 45° in all planes of the X, Y, and Z axis, where the roughness value Sz in area A varies from 259.50 µm. As a result, the orientation of the samples has no effect on roughness when measuring the Sz parameter.

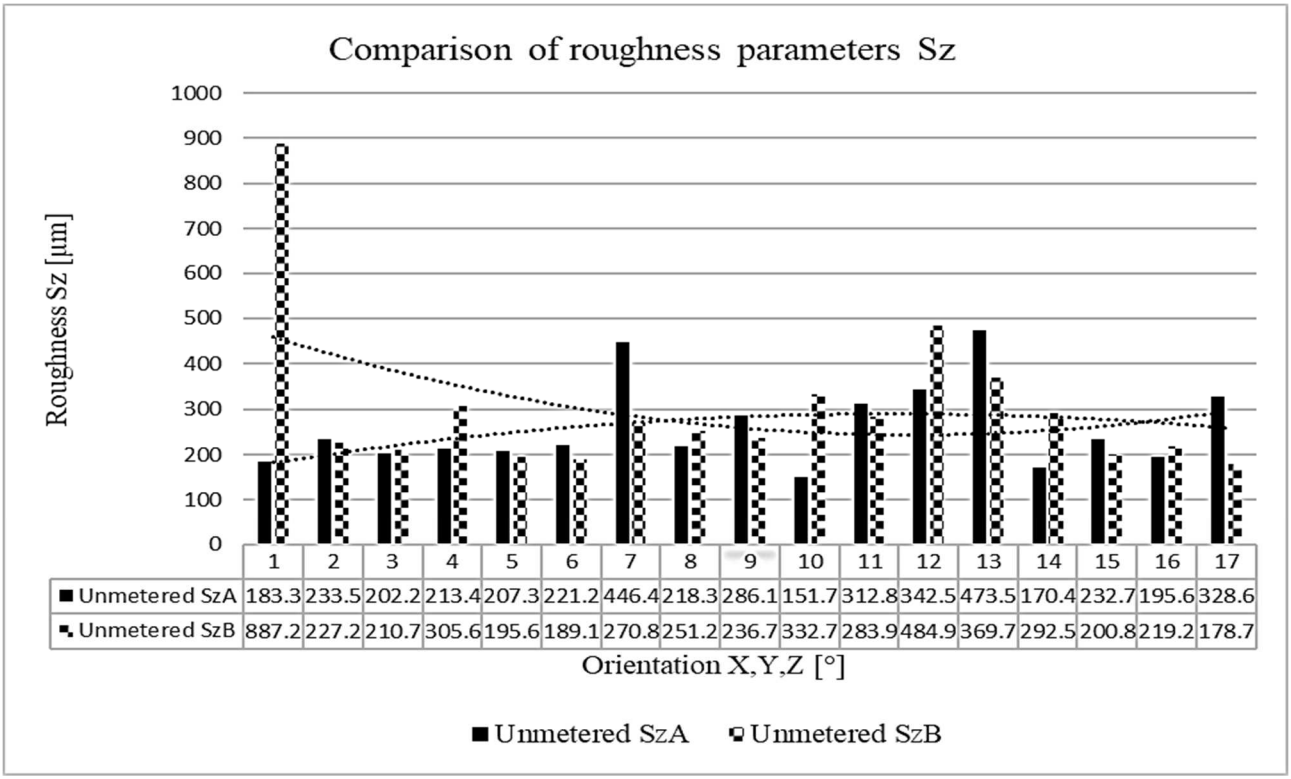

Fig. 4 *Graphical comparison of the results of measuring samples of the roughness parameter Sz*

Figure 5 compares selected surface roughness parameters evaluated by the Alicona InfiniteFocus G5 device for areas A and B. Within area A, the surface of sample no.1 was the best. The worst surface was measured on sample no. 12, and sample no. 6 also showed a higher measured value. This is a certain defect that occurs when the reprocessed powder is used. The reason for such a surface structure is the quality of the powder. Within area B, sample no. 1 had the best-measured surface, which had slightly higher measured values compared to area A. The highest measured value of surface roughness was on sample no. 12. Compared to area A, it had a better-measured surface roughness.

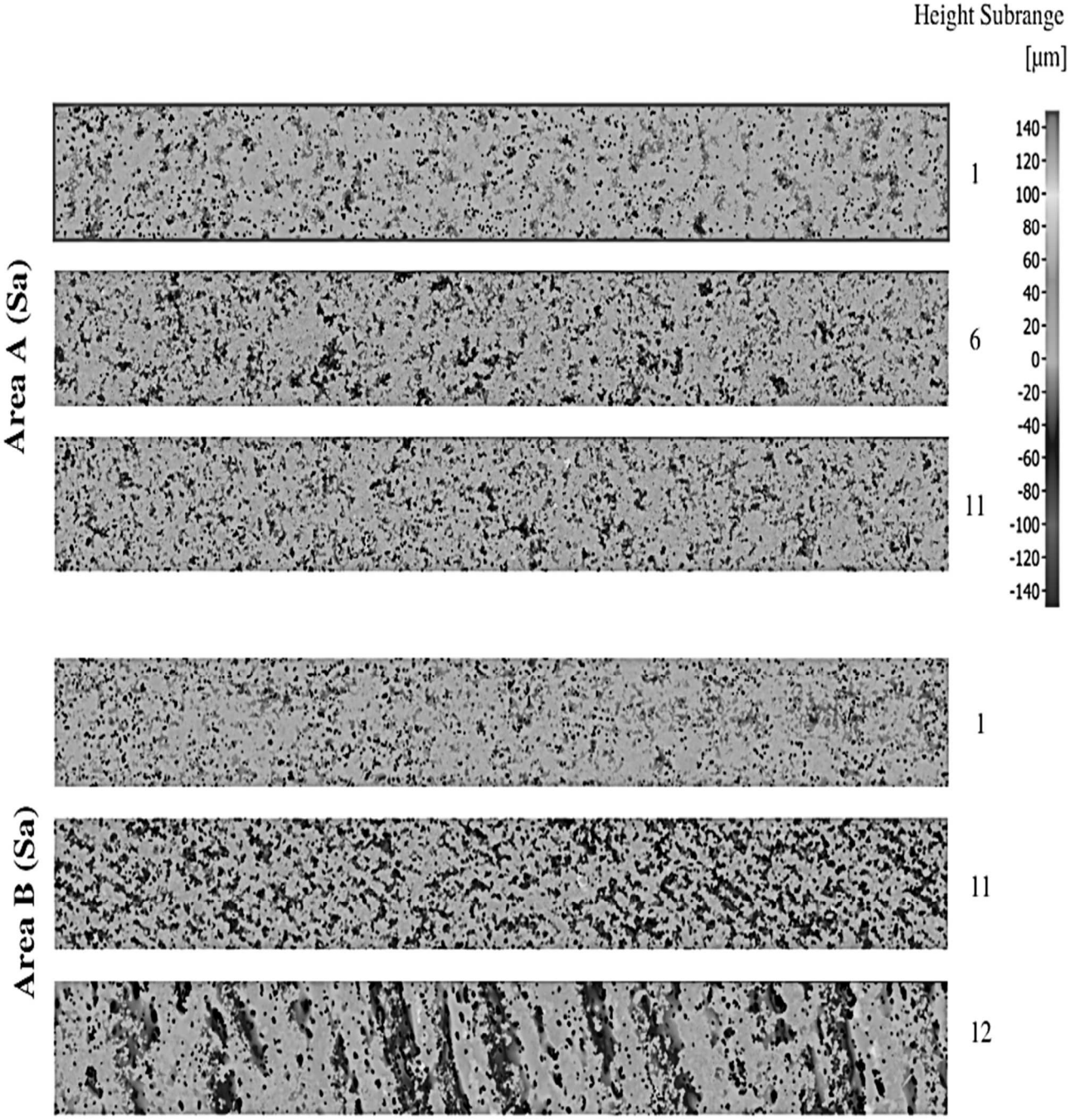

Fig. 5 *Selected parameters of surface roughness Sa within areas A and B*

3.2 Evaluation of Dimensional Accuracy

The places were measured repeatedly in the X, Y, and Z axes, with dimensions of 25x20x10 (Fig. 2), and the results were averaged. The measured values (Fig. 6) show that the values of the deviations measured on the X axis are predominantly positive, but the values of the deviations measured on the Y axis are half negative. We can see a link between sample 1 and the roughness parameter Sz, which was the highest within area B. The most accurate samples were 4, 7, and 8.

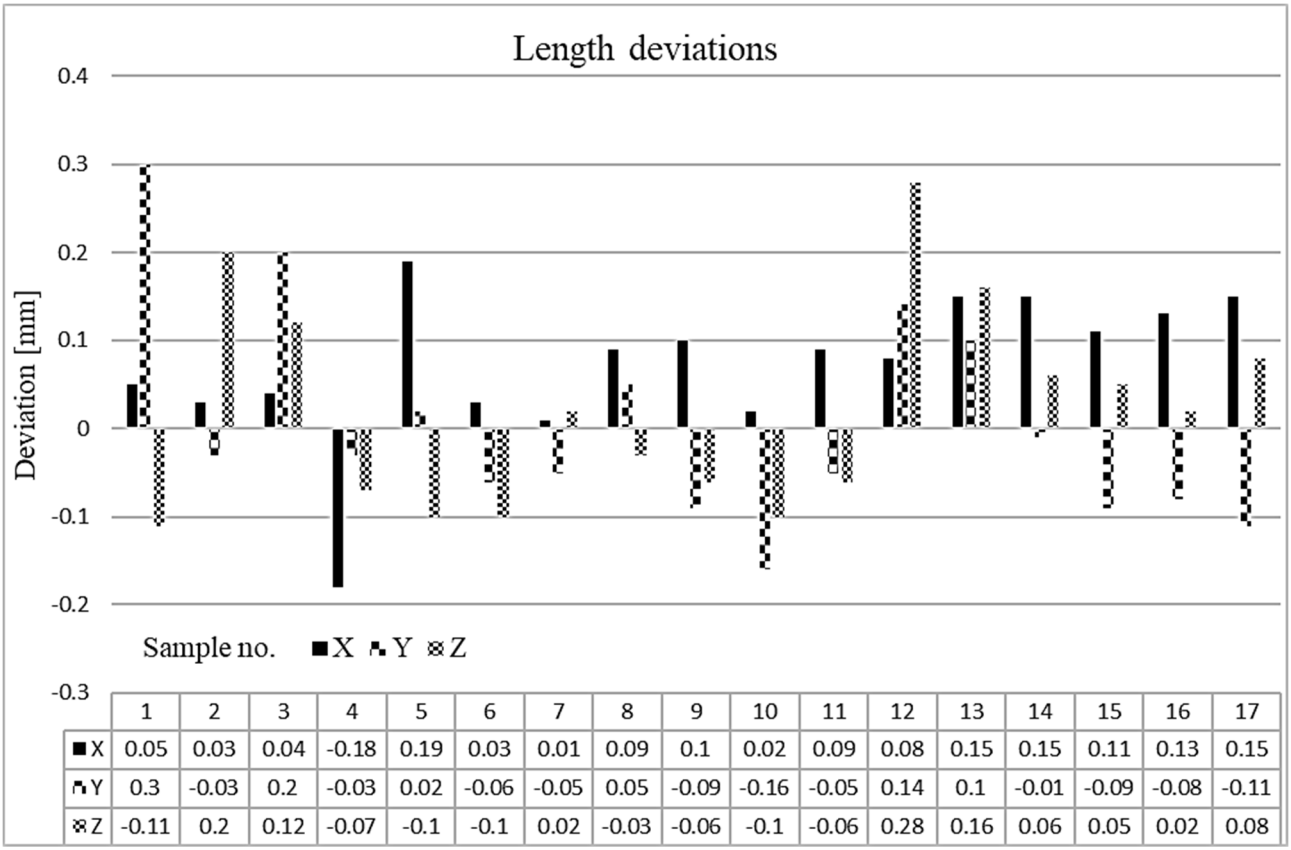

	1	2	3	4	5	6	7	8	9	10	11	12	13	14	15	16	17
X	0.05	0.03	0.04	-0.18	0.19	0.03	0.01	0.09	0.1	0.02	0.09	0.08	0.15	0.15	0.11	0.13	0.15
Y	0.3	-0.03	0.2	-0.03	0.02	-0.06	-0.05	0.05	-0.09	-0.16	-0.05	0.14	0.1	-0.01	-0.09	-0.08	-0.11
Z	-0.11	0.2	0.12	-0.07	-0.1	-0.1	0.02	-0.03	-0.06	-0.1	-0.06	0.28	0.16	0.06	0.05	0.02	0.08

Fig. 6 *Measured deviations by a micrometer*

3.3 Discussion of results

According to the findings, the print quality is influenced by the orientation of the samples but also by the surrounding conditions. We can confirm that the orientation of the samples in the build chamber had an impact on the dimensional quality when analyzing the dimensional accuracy. The evidence is a statistical evaluation where optimization in the following experiment could improve the results. Dimensional accuracy is related to deformation and shrinkage, as well as thermal energy distribution. Several studies have confirmed that orientation has a significant impact when printing large parts. The experiment itself could have been affected by a significant temperature load and by the fact that the samples were not far enough apart.

The surface roughness evaluation results confirmed that the statistically selected factors have no effect on the surface. By comparing samples of the roughness of the Sa parameter, the average value achieved was 13.45 μm in area A and 20.31 μm in area B. Within area A, the Sz parameter averaged 259.50 μm whereas, within area B, it averaged 306.88 m. A graphical comparison of the prints showed that the top surface A of the samples achieved better results than the side surface B.

The results of the dimensional accuracy measurement were reflected in the statistical dependence of factors on the measured values of dimensions, as well as a graphical comparison of dimension deviations, with the samples in the X-axis achieving the greatest deviation from the prescribed dimension on average. The surface roughness evaluation results confirm that the statistically selected factors have no effect on the surface. The graphical comparison of the samples shows that the top surface of the samples achieved better results than the side surface of the samples.

4 Conclusion

The aim of this study was to investigate the correlation between the geometry and surface properties of the printed samples at different rotation angles of the model in the X, Y and Z axes of the Cartesian coordinate system. For 17 specimens, the design and the results obtained were analyzed in Minitab statistical software using the DOE experimental method. The software demonstrated the dependence of the factors on the variable of interest.

To determine the surface quality for objective evaluation, the parameters Sa and Sz were determined. The tested surfaces were unmachined to determine which factors of the print setup conditions have the greatest influence on the resulting print quality. In addition to roughness, the dimensional accuracy of the 25x20x10 sample in the X, Y, and Z axes was also evaluated. The results revealed that the orientation of the specimens in the build chamber has an effect on

the dimensional accuracy, which depends on the uniform distribution of thermal energy. The specimens may have been subjected to significant thermal loading and were not sufficiently spaced apart. The ambient conditions and their effect on the resulting print quality, as well as measurement inaccuracies when the two-point method was not sufficient, contributed significantly to the poor model values. Reprocessed powder from previous prints also had a significant effect on the results that caused too much noise. Graphical comparison of the results reveals these inaccuracies, with no correlation between area and dimensions found. The results obtained in the present study can be helpful in preventing problems in the additive manufacturing process from polymer powders and also can be used in additive manufacturing for the specific type of printer and material used in further research.

Acknowledgement

This publication is the result of support under the Operational Program Integrated Infrastructure for the project: Strategic implementation of additive technologies to strengthen the intervention capacities caused by the COVID-19 pandemic ITMS code: 313011ASY4, co-financed by the European Regional Development Fund.

References

[1] KABIR, S.M.F., MATHUR, K., SEYAM, A.F.M. (2020). A critical review on 3D printed continuous fiber-reinforced composites: History, mechanism, materials and properties, In: *Composite Structures,* Vol. 232: 111476. https://doi.org/10.1016/j.compstruct.2019.111476

[2] STAVROPOULOS, P., FOTEINOPOULOUS, P. (2018). Modelling of additive manufacturing processes: A review and classification, In: *Manufacturing Review,* Vol. 5, No. 2. https://doi.org/10.1051/mfreview/2017014

[3] WANG, X., JIANG, M., ZHOU, Z., GOU, J., HUI, D. (2017). 3D printing of polymer matrix composites: A review and prospective, In: *Composites Part B: Engineering,* Vol. 110, pp. 442–458. https://doi.org/10.1016/J.COMPOSITESB.2016.11.034

[4] CAI, C., TEY, W.S., CHEN, J., ZHOU, W., LIU, X., LIU, T., ZHAO, L., ZHOU, K. (2021). Comparative study on 3D printing of polyamide 12 by selective laser sintering and multi jet fusion, In: *Journal of Materials Processing Technology,* Vol: 288: 116882. https://doi.org/10.1016/j.jmatprotec.2020.116882

[5] FINA, F., GOYANES, A., GAISFORD, S., BASIT, A.W. (2017). Selective laser sintering (SLS) 3D printing of medicines, In: *International journal of pharmaceutics,* Vol. 529, No. 1-2, pp. 285–293. https://doi.org/10.1016/j.ijpharm.2017.06.082

[6] DE OLIVEIRA SETTI, G., DE OLIVEIRA, M.F., MAIA, I.A., DA SILVA, J.V.L., SAVU, R., JOANNI, E. (2014). Correlation between mechanical and surface properties of SLS parts, In: *Rapid Prototyping Journal*, Vol. 20, No. 4, pp. 285–290. https://doi.org/10.1108/RPJ-08-2012-0070

[7] TOMANIK, M., ŻMUDZINSKA, M., WOJTKOV, M. (2021). Mechanical and structural evaluation of the PA12 desktop selective laser sintering printed parts regarding printing strategy. In: *3D Printing and Additive Manufacturing*, Vol. *8, No.* 4, pp. 271-279. https://doi.org/10.1089/3dp.2020.0111

[8] WI, K., SURESH, V., WANG, K., LI, B., QIN, H. (2019). Quantifying quality of 3D printed clay objects using a 3D structured light scanning system, In: *Additive Manufacturing*, Vol.32: 100987. https://doi.org/10.1016/j.addma.2019.100987

[9] DIZON, J. R. C., ESPERA Jr, A. H., CHEN, Q., ADVINCULA, R. C. (2018). Mechanical characterization of 3D-printed polymers. In: *Additive manufacturing*, Vol. *20*, pp. 44-67. https://doi.org/10.1016/j.addma.2017.12.002

[10] SACHDEVA, A., SINGH, S., SHARMA, V. S. (2013). Investigating surface roughness of parts produced by SLS process. In: *The International Journal of Advanced Manufacturing Technology*, Vol. 64, pp. 1505 - 1516. https://doi.org/10.1007/s00170-012-4118-z

[11] LAUNHARDT, M., WORZ, A., LODERER, A., LAUMER, T., DRUMMER, D., HAUSOTTE, T., SCHMIDT, M. (2016). Detecting surface roughness on SLS parts with various measuring techniques. In: *Polymer Testing*, Vol. *53*, pp. 217-226. https://doi.org/10.1016/j.polymertesting.2016.05.022

[12] DADBAKHS, S., VERBELEN, L., VERKINDEREN, O., STROBBE, D., VAN PUYVELDE, P., KRUTH, J. P. (2017). Effect of PA12 powder reuse on coalescence behav-

iour and microstructure of SLS parts. In: *European Polymer Journal*, Vol. *92*, pp. 250-262. https://doi.org/10.1016/j.eurpolymj.2017.05.014

[13] TYAGI, P., GOULET, T., RISO, C., STEPHENSON, R., CHUENPRATEEP, N., SCHLITZER, J., GARCIA-MORENO, F. (2019). Reducing the roughness of internal surface of an additive manufacturing produced 316 steel component by chempolishing and electropolishing. In: *Additive Manufacturing*, Vol. *25*, pp. 32-38.. https://doi.org/10.1016/j.addma.2018.11.001

[14] KLINGAA, C. G., DAHMEN, T., BAIER, S., MOHANTY, S., HATTEL, J. H. (2020). X-ray CT and image analysis methodology for local roughness characterization in cooling channels made by metal additive manufacturing. In: *Additive Manufacturing*, Vol. *32:* 101032. https://doi.org/10.1016/j.addma.2019.101032

[15] CUSTOMPART (2022). Selective Laser Sintering [online]. https://www.custompartnet.com/wu/selective-laser-sintering

[16] BĚHÁLEK, L. (2015). Polymery [online]. https://publi.cz/books/180/18.html

[17] YANG, F., ZOBEIRY, N., MAMIDALA, R., CHEN, X. (2022). A review of aging, degradation, and reusability of PA12 powders in selective laser sintering additive manufacturing. In: *Materials Today Communications*

[18] RAZAVIYE, M. K., TAFTI, R. A., KHAJEHMOHAMMADI, M. (2022). An investigation on mechanical properties of PA12 parts produced by a SLS 3D printer: An experimental approach. In: *CIRP Journal of Manufacturing Science and Technology*, Vol. *38*, pp. 760-768

[19] SINTERIT (2020) [online]. https://www.sinterit.com/wp-content/uploads/2020/12/Sinterit-Powders_Specification-PA12-Smooth.pdf

[20] MINITAB (2022). Design an experiment [online]. https://support.minitab.com/en-us/minitab/18/getting-started/designing-an-experiment/

[21] PETZOLD, S., KLETT, J., SCHAUER, A., OSSWALD, T.A. (2019). Surface roughness of polyamide 12 parts manufactured using selective laser sintering. In: *Polymer Testing,* Vol. 80 https://doi.org/10.1016/j.polymertesting.2019.106094

[22] OPTIMAX (2022). Alicona Infinite Focus G5+[online]. https://optimax-online.com/non-contact-metrology-3d-surface-characterisation/37/alicona-infinitefocus-g5+

[23] TIMKO, P., CZÁNOVÁ, T., CZÁN, A., SLABEJOVÁ, S., HOLUBJAK, J., CEDZO, M. (2022). Analysis of Parameters of Sintered Metal Components Created by ADAM and SLM Technologies. In: *Manufacturing Technology,* Vol. 22, No. 3, pp. 347-355. https:// 10.21062/mft.2022.032

[24] ROUDNICKA, M., VOJTECH, D., DANIEL, M. (2020). Aspects of Selective Laser Melting Technology Considered in the Preparation of Trabecular Structures for Bone Tissue Substitution. In: *Manufacturing Technology,* Vol. 20, No. 4, pp. 507-515. https:// 10.21062/mft.2022.065